

# Self-trapped quantum balls in binary Bose-Einstein condensates

**Sandeep Gautam**<sup>‡</sup>

Department of Physics, Indian Institute of Technology Ropar, Rupnagar,  
Punjab 140001, India

**S. K. Adhikari**<sup>§</sup>

Instituto de Física Teórica, Universidade Estadual Paulista - UNESP, 01.140-070  
São Paulo, São Paulo, Brazil

## **Abstract.**

We study the formation of a stable self-trapped spherical quantum ball in a binary Bose-Einstein condensate (BEC) with two-body inter-species attraction and intra-species repulsion employing the beyond-mean-field Lee-Huang-Yang and the three-body interactions. We find that either of these interactions or a combination of these can stabilize the binary BEC quantum ball with very similar stationary results, and for a complete description of the problem both the terms should be considered. These interactions lead to higher-order nonlinearities, e.g. quartic and quintic, respectively, in a nonlinear dynamical equation compared to the cubic nonlinearity of the two-body contact interaction in the mean-field Gross-Pitaevskii equation. The higher-order nonlinearity makes the energy infinitely large at the center of the binary ball and thus avoids its collapse. In addition to the formation of stationary binary balls, we also study a collision between two such balls. At large velocities, the collision is found to be elastic, which turns out to be inelastic as the velocity is lowered. We consider the numerical solution of a beyond-mean-field model for the binary ball as well as a single-mode variational approximation to it in this study.

<sup>‡</sup> sandeep@iitrpr.ac.in

<sup>§</sup> adhikari44@yahoo.com, <http://www.ift.unesp.br/users/adhikari>

## 1. Introduction

A one-dimensional (1D) matter-wave bright soliton, bound due to a balance between nonlinear attraction and defocusing forces, can travel at a constant velocity [1]. Solitons have been studied and observed in different classical and quantum systems, such as, on water surface, and in nonlinear optics [2] and Bose-Einstein condensate (BEC) [3]. In many cases, the 1D soliton is found to be analytic with momentum and energy conservation which guarantee elastic collision between solitons with shape preservation. In a BEC, quasi-1D solitons have been realized [3] in a cigar-shaped configuration with strong confining traps in transverse directions following a theoretical suggestion [4]. However, such a soliton cannot be realized [1, 2] in a three-dimensional (3D) system due to a collapse instability for attractive interaction.

The theoretical studies on BEC solitons are usually based on the mean-field Gross-Pitaevskii (GP) equation [5] with two-body contact interaction. It has been demonstrated that an inclusion of the beyond-mean-field Lee-Huang-Yang (LHY) interaction [6, 7] or of a three-body interaction [8] in the dynamical model, both leading to a higher-order repulsive nonlinear term compared to the cubic nonlinear two-body attraction in the GP equation, can arrest the collapse and lead to a self-bound BEC droplet. Petrov [7] demonstrated the formation of a binary BEC droplet for an intra-species repulsion with LHY interaction and an inter-species attraction. One of us [8] demonstrated the formation of a BEC quantum ball for an attractive two-body and a repulsive three-body interaction. We prefer the name quantum ball or simply ball over quantum *droplet* for the localized *nondipolar* BEC state after establishing the robustness of such a state to maintain the spherical ball-like shape after collision [8] in contrast to easily deformable liquid droplets. A binary boson-fermion quantum ball can be formed for an attractive boson-fermion and repulsive boson-boson interaction together with the LHY interaction and/or with a repulsive three-boson interaction [9], while the fermions remain quasi-noninteracting. A quantum ball can also be formed in a multi-component spinor BEC with spin-orbit or Rabi coupling [10]. The spin-orbit coupling and Raman coupling can also generate an effective interatomic repulsion cancelling the mean-field attraction and stabilizing the binary trapped condensates against collapse [11]. The exchange induced spin-orbit coupling, when only one of the component of the binary system is coupled with Raman lasers, has recently been studied [12]. There also has been suggestion for dynamically stabilized self-bound 3D states [13]. Quantum droplets were realized and studied in dipolar  $^{164}\text{Dy}$  [14] and  $^{166}\text{Er}$  [15] BECs. The formation of dipolar droplets was later explained by including an LHY interaction [16, 17, 18, 19, 20] or a three-body interaction [21] to the contact interaction. Following the suggestion of Petrov [7], more recently, a binary BEC ball of two hyperfine states of  $^{39}\text{K}$  for attractive inter-species and repulsive intra-species interactions has been observed [22, 23, 24].

In the previous studies of quantum droplets in dipolar [16, 18, 19, 20] and binary [22, 23, 24] BECs, the LHY interaction was considered to be responsible for binding. The LHY interaction leads to a higher-order repulsive quartic nonlinearity in the dynamical model compared to the cubic nonlinearity of the GP equation arising from the two-body contact interaction in the Hartree approximation. In fact, any higher-order repulsive nonlinearity, or their combination, can stabilize the droplet.

In this study, we consider a repulsive three-body interaction together with the LHY interaction for the formation of a stable self-bound spherical binary BEC quantum ball with repulsive intra-species and attractive inter-species interaction.

We find that either the LHY interaction or a repulsive three-body interaction or a combination of both can stabilize the binary ball with very similar results, and for a complete description of the problem both the terms should be considered. Without these higher-order terms, an attractive BEC has an infinite negative energy at the center leading to a collapse of the system to the center. Any higher-order repulsive term, however small it may be, leads to an infinite positive energy at the center and stops the collapse.

We consider a binary  $^{87}\text{Rb}$  system in two different hyperfine states. We derive the binary model equations with the LHY interaction and a repulsive three-body term and solve it numerically without approximation. In addition, we consider a variational approximation [25] to our model in a single-mode approximation (SMA) when the binary set of equations is reduced to a single equation. The SMA is commonly used [26] in a description of a spinor BEC. Two different variational *ansatz* – a Gaussian and a modified Gaussian – were used for a better approximation to the density profile. In addition to the formation of stationary binary balls, we also considered moving balls and collisions between two such balls. At high velocities, the collision was found to be essentially elastic with practically no deformation. At lower velocities, the collision turns inelastic.

In Sec. 2.1 we derive the binary model nonlinear Schrödinger (NLS) equations appropriate for this study. To make these equations, with complicated nonlinear terms, analytically tractable, we consider a SMA in Sec. 2.2. A Gaussian variational approximation is then implemented on the model SMA equation. Numerical results of the model using the split time-step Crank-Nicolson [27] and Fourier pseudo-spectral [28] methods for stationary binary balls are presented in Sec. 3.1 and compared with variational results. In Sec. 3.2 the numerical results for collision dynamics of two binary balls are considered. A summary and discussion of the study is presented in Sec. 4.

## 2. Analytical Result

### 2.1. Binary model equations

The interaction energy density  $\mathcal{E}$  (energy per unit volume) of a homogeneous dilute weakly repulsive Bose gas with LHY interaction [6] as well as two and three-body interactions is given by [7, 8]

$$\mathcal{E} = \frac{Un^2}{2} \left( 1 + \frac{128\sqrt{na^3}}{15\sqrt{\pi}} \right) + K_3 \frac{n^3}{6}, \quad (1)$$

$$= \frac{Un^2}{2} + \frac{8m^4}{15\pi^2\hbar^3} c^5 + K_3 \frac{n^3}{6}, \quad (2)$$

where  $n$  is the number density, the two-body interaction strength  $U = 4\pi\hbar^2 a/m$ ,  $a$  is the s-wave scattering length,  $m$  is the mass of an atom,  $K_3$  is the three-body interaction strength,  $c = \sqrt{Un/m}$  is the speed of sound in the single component BEC [5, 31]. The first two terms on the right-hand-side (rhs) of (2) are the two-body interaction and its LHY correction, respectively, and the last term is the three-body interaction. The LHY interaction is equal to the zero point energy of the Bogoliubov modes [7]. The bulk chemical potential  $\mu \equiv \partial\mathcal{E}/\partial n$  is the nonlinear interaction term of the following

time-dependent mean-field NLS equation for a trapped BEC:

$$i\hbar \frac{\partial \psi}{\partial t} = \frac{-\hbar^2 \nabla^2}{2m} \psi + V\psi + U|\psi|^2 \left( 1 + \frac{32a^{3/2}|\psi|}{3\sqrt{\pi}} \right) \psi + \frac{K_3}{2} |\psi|^4 \psi, \quad (3)$$

where  $V$  is the trapping potential,  $\psi(\mathbf{r}, t)$  is the condensate wave function and, in terms of it, condensate density  $n(\mathbf{r}) = |\psi(\mathbf{r})|^2$  with the normalization  $\int |\psi|^2 d\mathbf{r} = N$ , where  $N$  is the number of trapped atoms in the BEC.

The beyond-mean-field LHY energy contribution to energy, viz. (2), has limited validity for only small scattering lengths [29]. For larger scattering lengths, specially at unitarity as  $a \rightarrow \infty$ , this term diverges even faster than the GP term proportional to scattering length, while the energy density should be finite. An analytic beyond-mean-field energy density valid for both small and large scattering lengths has been given [30]. However, for values of scattering lengths considered in this study the LHY expression (2) gives the actual state of affairs.

In a binary BEC, there are two speeds of sound  $c_i$  [31], where suffix  $i = 1, 2$  identifies the two species of atoms, and the energy density with LHY and three-body interactions in a homogeneous medium is [32]

$$\mathcal{E} = \sum_i \left[ \frac{U_i n_i^2}{2} + \frac{8m^4}{15\pi^2 \hbar^3} c_i^5 \right] + U_{12} n_1 n_2 + \frac{K_3}{6} n^3, \quad (4)$$

where  $n = n_1 + n_2$ . Here intra-species and inter-species three-body interaction strengths and masses are taken to be equal to  $K_3$  and  $m$ , respectively, the two-body intra- and inter-species interaction strengths are  $U_i = 4\pi\hbar^2 a_i/m$  with  $a_i$  the  $s$ -wave intra-species scattering length for species  $i$ , and  $U_{12} = 4\pi\hbar^2 a_{12}/m$ , where  $a_{12}$  is the  $s$ -wave inter-species scattering length, respectively. The two speeds of the sound for the system are [31, 33]

$$c_{\pm} = \sqrt{\frac{\sum_i U_i n_i \pm \sqrt{(U_1 n_1 - U_2 n_2)^2 + 4n_1 n_2 U_{12}^2}}{2m}}. \quad (5)$$

If  $U_{12} \approx -\sqrt{U_1 U_2}$  for repulsive intra-species and attractive inter-species interactions,  $c_- \approx 0$  and  $c_+ \approx \sqrt{(U_1 n_1 + U_2 n_2)/m}$ . Then, the mean field energy with LHY and three-body interactions can be written as

$$\mathcal{E} = \sum_i \frac{U_i n_i^2}{2} + U_{12} n_1 n_2 + \frac{8m^4}{15\pi^2 \hbar^3} \left( \frac{\sum_i U_i n_i}{m} \right)^{5/2} + \frac{K_3}{6} n^3. \quad (6)$$

In this case the chemical potentials  $\mu_i \equiv \partial \mathcal{E} / \partial n_i$  are the nonlinear terms of the following binary time-dependent NLS equation for the localized BEC mixture

$$i\hbar \frac{\partial \psi_1}{\partial t} = \left[ \frac{-\hbar^2 \nabla^2}{2m} + V + U_1 |\psi_1|^2 + U_{12} |\psi_2|^2 + \frac{K_3}{2} \left( \sum_i |\psi_i|^2 \right)^2 + \frac{32U_1 (\sum_i a_i |\psi_i|^2)^{3/2}}{3\sqrt{\pi}} \right] \psi_1, \quad (7)$$

$$i\hbar \frac{\partial \psi_2}{\partial t} = \left[ \frac{-\hbar^2 \nabla^2}{2m} + V + U_2 |\psi_2|^2 + U_{12} |\psi_1|^2 + \frac{K_3}{2} \left( \sum_i |\psi_i|^2 \right)^2 + \frac{32U_2 (\sum_i a_i |\psi_i|^2)^{3/2}}{3\sqrt{\pi}} \right] \psi_2, \quad (8)$$

with  $n_i(\mathbf{r}) = |\psi_i(\mathbf{r})|^2$  and  $\int |\psi_i|^2 d\mathbf{r} = N_i$ , where  $N_i$  is the number of atoms in species  $i$ .

Let us define  $l_0 \equiv 1 \mu\text{m}$  as a scaling length which we use to rewrite the (7)-(8) in dimensionless form. To this end, we write length, number density, time, and energy in the units of  $l_0$ ,  $l_0^{-3}$ ,  $ml_0^2/\hbar$ , and  $\hbar^2/ml_0^2$ , respectively. The dimensionless version of (7)-(8) thus obtained is

$$i\frac{\partial\phi_1}{\partial\tilde{t}} = \left[ \frac{-\tilde{\nabla}^2}{2} + \tilde{V} + \tilde{U}_1|\phi_1|^2 + \tilde{U}_{12}|\phi_2|^2 + \frac{\tilde{K}_3}{2} \left( \sum_i N_i |\phi_i|^2 \right)^2 + \frac{16\tilde{a}_1 (\sum_i U_i |\phi_i|^2)^{3/2}}{3\pi} \right] \phi_1, \quad (9)$$

$$i\frac{\partial\phi_2}{\partial\tilde{t}} = \left[ \frac{-\tilde{\nabla}^2}{2} + \tilde{V} + \tilde{U}_2|\phi_2|^2 + \tilde{U}_{21}|\phi_1|^2 + \frac{\tilde{K}_3}{2} \left( \sum_i N_i |\phi_i|^2 \right)^2 + \frac{16\tilde{a}_2 (\sum_i U_i |\phi_i|^2)^{3/2}}{3\pi} \right] \phi_2, \quad (10)$$

where the dimensionless variables are defined by  $|\phi_i|^2 = N_i^{-1} |\psi_i|^2 l_0^3$ ,  $\tilde{U}_i = 4\pi N_i \tilde{a}_i$ ,  $\tilde{U}_{12} = 4\pi N_2 \tilde{a}_{12}$ ,  $\tilde{U}_{21} = 4\pi N_1 \tilde{a}_{12}$ ,  $\tilde{K}_3 = mK_3/(\hbar l_0^4)$ . The normalization conditions satisfied by the dimensionless wave functions now are  $\int |\phi_i|^2 d\tilde{\mathbf{r}} \equiv \int \tilde{n}_i d\tilde{\mathbf{r}} = 1$ . To simplify the notation, we will denote the dimensionless variables without tilde except if stated otherwise. All the symbols used in the rest of the paper are dimensionless. In the following, for the formation of a self-trapped binary ball we will set the trapping potential  $V = 0$ .

## 2.2. Single-Mode Variational Approximation

The Lagrangian density of the spherical binary ball with LHY and three-body interactions is

$$\mathcal{L} = \sum_i \frac{N_i}{2} \left\{ i(\phi_i \phi_i^{*\prime} - \phi_i^* \phi_i') + |\nabla \phi_i|^2 + U_i |\phi_i|^4 \right\} + N_1 U_{12} |\phi_1|^2 |\phi_2|^2 + \frac{8(\sum_i U_i |\phi_i|^2)^{5/2}}{15\pi^2} + \frac{K_3 (\sum_i N_i |\phi_i|^2)^3}{6}, \quad (11)$$

where prime denotes time derivative. Equations (9) and (10) are the Euler-Lagrange equations of this Lagrangian density. The energy density  $\mathcal{E}$  of a stationary state is the same as the Lagrangian density  $\mathcal{L}$  setting the time-derivatives to zero.

To make the Lagrange variational analysis [25] analytically tractable, we use single-mode approximation (SMA), which implies that both the component wave functions have the same shape. Indeed, in our numerical calculation we find that in many cases the component densities are very similar. Here we formulate a simple variational approximation in these cases. In the present case, where the dimensionless wave functions are normalized to unity, SMA means  $|\phi_1|^2 = |\phi_2|^2$ .

In a localized system, when  $a_{12} = -\sqrt{a_1 a_2}$ , which implies that  $\sqrt{N_1} U_{12} = -\sqrt{N_2} \sqrt{U_1 U_2}$ , the mean-field interaction energy density without LHY and three-body interactions is

$$\mathcal{E}_{\text{int}} = \frac{1}{2} \left[ \sqrt{N_1 U_1} n_1 - \sqrt{N_2 U_2} n_2 \right]^2, \quad (12)$$

where  $n_i = |\phi_i|^2$ . Minimizing interaction energy density (12) with respect to densities  $n_1$  and  $n_2$ , we get

$$N_1\sqrt{a_1}n_1 = N_2\sqrt{a_2}n_2. \quad (13)$$

Equation (13) implies that if  $N_1\sqrt{a_1} = N_2\sqrt{a_2}$ , then  $|\phi_1|^2 = |\phi_2|^2$ , which is the condition for SMA. Hence if we assume  $a_{12} \approx -\sqrt{a_1a_2}$  and choose  $N_1\sqrt{a_1} = N_2\sqrt{a_2}$ , SMA will be a reasonable approximation even after including the LHY and three-body interactions. Nevertheless, for the formation of a self-bound binary ball we require an attractive two-body energy density, which is possible for  $a_{12} < -\sqrt{a_1a_2}$ . To satisfy this condition, we take  $a_{12} = -(\delta a + \sqrt{a_1a_2})$ , where we take  $\delta a$  to be small and positive so that the condition of SMA remains approximately valid. Thus setting  $|\phi| \equiv |\phi_i|, i = 1, 2$ , the Lagrangian density (11) becomes

$$\begin{aligned} \mathcal{L} = & \frac{N}{2} \left\{ i(\phi\phi^{*\prime} - \phi^*\phi') + |\nabla\phi|^2 \right\} - 4\pi N_1 N_2 \delta a |\phi|^4 \\ & + \frac{256\sqrt{\pi}}{15} \left( \sum_i N_i a_i \right)^{5/2} |\phi|^5 + \frac{K_3}{6} N^3 |\phi|^6, \end{aligned} \quad (14)$$

where  $N = N_1 + N_2$ . This Lagrangian density with the time-derivative terms and  $K_3$  set equal to zero is the same as the stationary energy density given by (1) of Ref. [22]. The NLS equation in the SMA is the following Euler-Lagrange equation of Lagrangian density (14):

$$\begin{aligned} i\frac{\partial\phi}{\partial t} = & \left[ -\frac{\tilde{\nabla}^2}{2} - \frac{8\pi N_1 N_2}{N} \delta a |\phi|^2 + \frac{K_3}{2} N^2 |\phi|^4 \right. \\ & \left. + \frac{128\sqrt{\pi} \left( \sum_i N_i a_i \right)^{5/2}}{3N} |\phi|^3 \right] \phi. \end{aligned} \quad (15)$$

A Lagrange variational approximation to the SMA (15) can be performed with the following variational *ansatz* [25]

$$\phi = \pi^{-3/4} w^{-3/2} \exp\left(-\frac{r^2}{2w^2} + i\kappa r^2\right), \quad (16)$$

where  $w$  is the width and  $\kappa$  the chirp. Although we are looking for a real density, the wave function is complex and has a phase. The chirp term is a simple way of introducing the phase. This term is necessary to get the time-dependent dynamics, viz. Eq. (19). For a stationary solution we can set this term to zero. Using this *ansatz*, the Lagrangian density (14) can be integrated over all space to yield the Lagrangian functional

$$\begin{aligned} L \equiv \int \mathcal{L} d\mathbf{r} = & 3\kappa^2 w^2 N + \frac{3}{2} w^2 \kappa' N + \frac{3N}{4w^2} - \frac{8\pi N_1 N_2 \delta a}{4\sqrt{2}\pi^{3/2} w^3} \\ & + \frac{512\sqrt{2} \left( \sum_i N_i a_i \right)^{5/2}}{75\sqrt{5}\pi^{7/4} w^{9/2}} + \frac{K_3 N^3}{18\sqrt{3}\pi^3 w^6}, \end{aligned} \quad (17)$$

where for this study of a self-trapped binary ball, we have removed the contribution of the trapping potential  $V$ . If  $w$  is the characteristic size of the condensate, the kinetic energy, interaction energy, LHY interaction energy, and three-body interaction energy scale as  $w^{-2}$ ,  $-w^{-3}$ ,  $w^{-9/2}$ , and  $w^{-6}$ , respectively. This energy scaling suggests that a minimum in energy (local or global) can occur for a finite size  $w$ . This vindicates the use of variational *ansatz* (16) having a characteristic width  $w$  like a Gaussian function, specially for the tightly bound balls. Nevertheless the homogeneous equation (15)

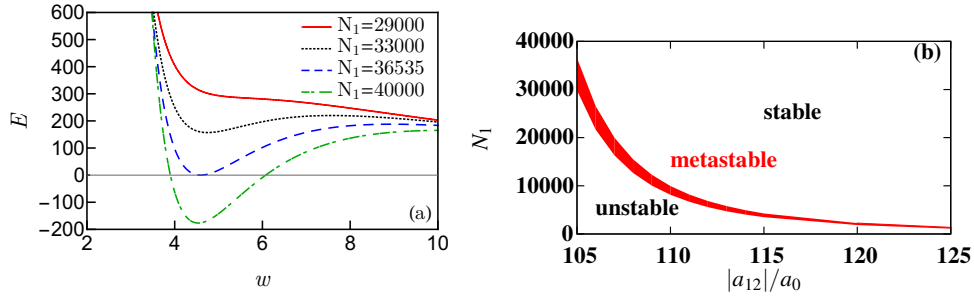


**Figure 1.** (a) Variational energy of a binary stationary Rb<sup>87</sup> ball with  $a_{12} = -105a_0$  and  $N_1 = 29000, 33000, 36535, 40000$  as a function of the width of the condensate. (b) Phase plot in  $N_1 - |a_{12}|$  plane showing the formation of a stable and meta-stable binary ball. Other parameters used are  $a_1 = 100.4a_0$ ,  $a_2 = 95a_0$ ,  $K_3 = 1.8 \times 10^{-41} \text{ m}^6/\text{s}$ , and  $N_2 = N_1 \sqrt{a_1/a_2}$ . The plotted quantities in this and following figures are dimensionless.

(setting the non-linear terms to zero) is a plane-wave equation. Using the definition of Fourier transform the Gaussian ansatz (16) can be considered as the superposition of an infinite number of plane waves. This justifies the use of a Gaussian ansatz in Eq. (15).

In the absence of the last two terms in Eq. (17) with LHY and three-body energy contributions, the Lagrangian (or the energy) of a stationary state obtained by setting  $\kappa = 0$  in (17) tends to  $-\infty$  as  $w \rightarrow 0$  signaling a collapse instability. However, in the presence of any or both of these terms the energy at the center ( $w = 0$ ) becomes infinitely large and hence a collapse is avoided. The Euler-Lagrange equations of the Lagrangian (17) for variable  $\nu \equiv \kappa, w$ ,

$$\frac{\partial}{\partial t} \frac{\partial L}{\partial \nu'} - \frac{\partial L}{\partial \nu} = 0, \quad (18)$$

lead to

$$w'' = \frac{1}{w^3} - \frac{4\pi N_1 N_2 \delta a}{\sqrt{2}\pi^{3/2} w^4 N} + \frac{512\sqrt{2} (\sum_i N_i a_i)^{5/2}}{25\sqrt{5} N \pi^{7/4} w^{11/2}} + \frac{2K_3 N^2}{9\sqrt{3}\pi^3 w^7}, \quad (19)$$

which describes the variation of the width of the condensate with time. The width of a stationary binary ball is obtained by setting  $w'' = 0$  in (19).

### 3. Numerical Result

We use split time-step Fourier pseudo-spectral method to solve the coupled NLS equations (9)-(10) numerically [28]. We also cross-checked our results with split time-step Crank-Nicolson method [27]. The minimum-energy ground-state solution for the binary ball is obtained by evolving the trial wave functions, chosen to be Gaussian, in imaginary time  $\tau = it$  using (9)-(10) as is proposed in Refs. [27]. In numerical calculation we employ periodic boundary condition, and the size of numerical domain is taken sufficiently larger than the typical size of the self-trapped solution to make the boundary effects to be negligible. The numerical results of the model for stationary binary balls presented in Sec. 3.1 are obtained using spherical coordinate  $r$ . The spatial and time steps used to solve the NLS equations in imaginary time are  $r = 0.0025$  and  $t = 3.125 \times 10^{-6}$ . We consider a binary ball consisting of

$|F = 1, m_F = +1\rangle$  and  $|F = 2, m_F = -1\rangle$  hyperfine states of  $^{87}\text{Rb}$ , which has been realized experimentally [34]. We term these as components 1 and 2, respectively, in the rest of the paper. The intra-species  $s$ -wave scattering lengths of the two components are  $a_1 = 100.4a_0$  and  $a_2 = 95a_0$  for components 1 and 2, respectively [34], with  $a_0$  the Bohr radius. The inter-species scattering length for the system  $a_{12}$  is tunable with a magnetic Feshbach resonance [35], and can thus be used to realize the quantum ball. The collision dynamics of the moving binary balls is studied by real-time propagation in Cartesian coordinates with space and time steps 0.04 and 0.0004, respectively, using the initial states obtained by imaginary-time propagation.

### 3.1. Stationary quantum balls

We consider the formation of a binary stationary quantum ball of  $^{87}\text{Rb}$  atoms in two hyperfine states with  $N_1 = 30000$  and  $50000$  atoms in the first state. The number of atoms in the second state is taken as  $N_2 = N_1\sqrt{a_1/a_2}$  (chosen to make SMA a good approximation). The inter-species scattering length is taken as  $a_{12} = -105a_0$ . The scaling length used to write dimensionless NLS equation is  $l_0 = 1 \mu\text{m}$ ; the corresponding scaling time is  $ml_0^2/\hbar = 1.37$  ms. Actually, there is no estimate of  $K_3$ , the three-body interaction strength and specially, its real part, which helps in the formation of the binary ball. However, an estimate for the three-body loss rate – the imaginary part of  $K_3$  – of  $^{87}\text{Rb}$  exists:  $K_3 = 1.8 \times 10^{-41} \text{ m}^6/\text{s}$  [34, 36]. Because of unitarity constraints the real part of  $K_3$  should have a magnitude of the same order. In this study we take the real and imaginary parts of  $K_3$  to be identical, e.g.,  $K_3 = 1.8 \times 10^{-41}(1 - i) \text{ m}^6/\text{s}$ . Nevertheless, in the study of the stationary quantum ball we set the imaginary part of  $K_3$  to zero, and later we find in the study of dynamics that the effect of the imaginary part is negligible. The numerical solution for the ground-state binary ball is obtained by imaginary-time propagation and the variational solution is obtained from a solution of (19) with  $w'' = 0$ .

The variational results confirm the existence of energetically meta-stable as well as stable balls. To illustrate the distinction between a meta-stable and a stable ball, the variational energy  $E$  of binary balls with aforementioned scattering lengths as a function of the variational width  $w$  are plotted in figure 1(a). Incidentally, the variational energy  $E$  is the Lagrangian (17) with  $\kappa = 0$ . In figure 1(a), a meta-stable ball corresponds to a curve with a local minimum in the energy, whereas a stable ball corresponds to the curve with a global minimum. These two cases are shown in figure 1(a) for  $N_1 = 33000$  and  $N_1 = 40000$ , respectively. An unstable ball corresponds to a curve with no minimum, viz.  $N_1 = 29000$  in figure 1(a). The variational phase plot of the system in the  $N_1 - |a_{12}|$  plane, while keeping intra-species scattering lengths and  $K_3$  fixed, is shown in figure 1(b), which clearly shows the regions of energetically stable and meta-stable balls. In the following we will study only the stable binary balls.

In figures 2(a)-(d), we display the numerical and variational common densities  $|\phi_j|^2$  with  $j = 1, 2$  of the two components of the binary ball for different parameters. The variational result with SMA (19) is in good agreement with the numerical solution of the NLS equations (9)-(10) with LHY and three-body interactions as is shown in figures 2(a)-(b). In figures 2(c)-(d), density profiles of the binary ball after switching off the LHY interaction are also shown. The variational densities in this case are poor approximations to the numerical ones. This is due to the fact that in the absence of the LHY interaction, the repulsive force needed for the stabilization of the quantum ball



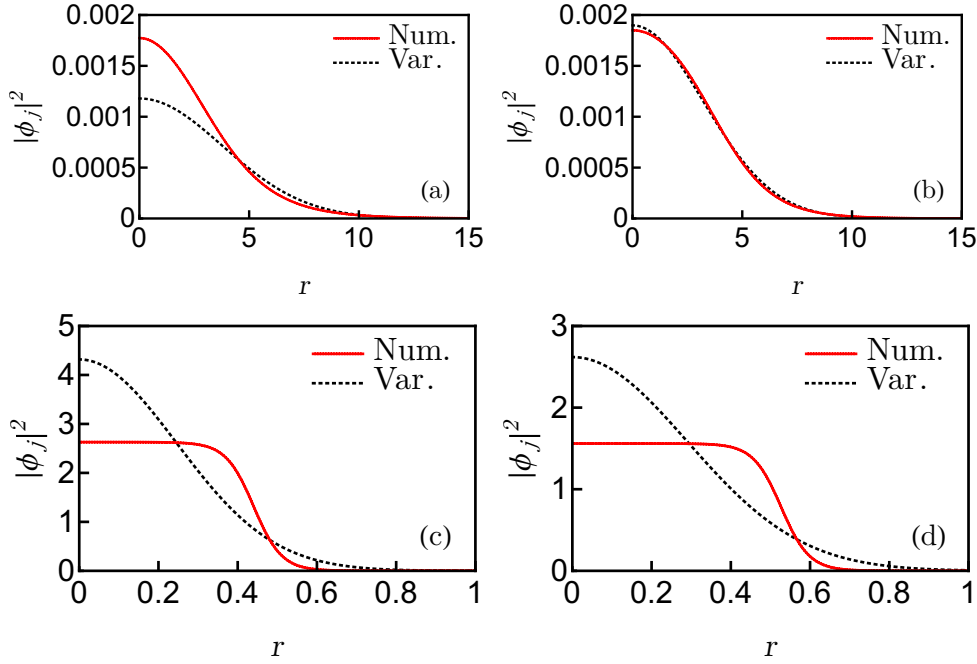


**Figure 2.** Numerical (Num.) and variational (Var.) density of a binary  $^{87}\text{Rb}$  ball with  $a_1 = 100.4a_0$ ,  $a_2 = 95a_0$ ,  $a_{12} = -105a_0$ ,  $K_3 = 1.8 \times 10^{-41} \text{ m}^6/\text{s}$ , and  $N_2 = N_1 \sqrt{a_1/a_2}$  for (a)  $N_1 = 30000$ , and (b)  $N_1 = 50000$ . (c) and (d) display the densities for the same parameters as in (a) and (b), respectively, but with the LHY interaction switched off.

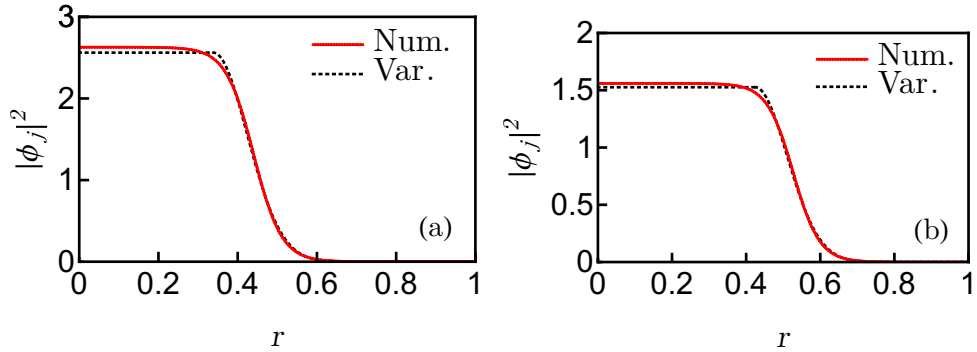


**Figure 3.** Numerical (Num.) and variational (Var.) density of a binary  $^{87}\text{Rb}$  ball for (a)  $N_1 = 30000$  and (b)  $N_1 = 50000$ . All other parameters are the same as in figure 2(c) and (d), respectively. Variational results are calculated with *ansatz* (20).

is provided by the kinetic energy and the three-body interaction. If the characteristic width of the ball  $w \ll 1$ , then the three-body interaction energy, which varies as  $w^{-6}$ , is much larger than the kinetic energy, which varies as  $w^{-2}$ , as is evident from their respective contributions in the Lagrangian (17). Therefore to model the densities, in

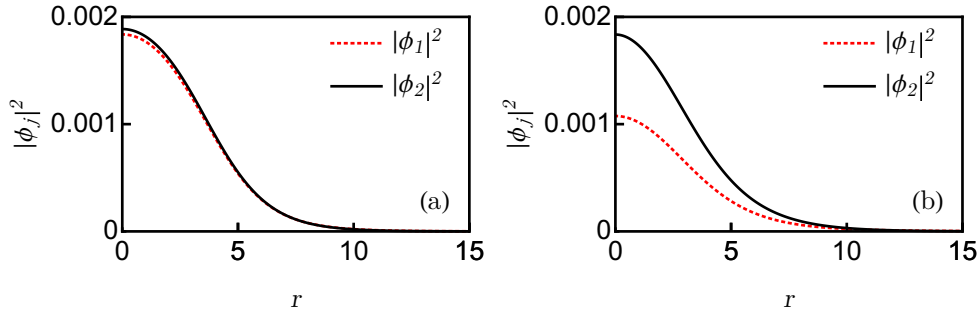


**Figure 4.** Numerical density of a binary  $^{87}\text{Rb}$  ball with (a)  $N_1 = N_2 = 50000$ , and (b)  $N_1 = 50000$ ,  $N_2 = 30000$ . Other parameters used are  $a_1 = 100.4a_0$ ,  $a_2 = 95a_0$ ,  $a_{12} = -105a_0$ , and  $K_3 = 1.8 \times 10^{-41} \text{ m}^6/\text{s}$ .

the absence of the LHY interaction for small  $K_3$ , one can neglect the kinetic energy in comparison to mean-field two- and three-body interaction energies, except near the surface of the ball, in the NLS equations (9)-(10). This will lead to constant density profiles for the components in the bulk of the binary ball. The kinetic energy nevertheless will contribute to the energy near the surface of the ball where the wave function would decay to zero over some length. This motivates the use of the following piece-wise continuous variational *ansatz* for the component densities

$$\phi_j(r) = \begin{cases} b, & 0 < r \leq R_{\text{in}} \\ b \exp\left[-\frac{(r-R_{\text{in}})^2}{2l^2}\right], & R_{\text{in}} \leq r < \infty, \end{cases} \quad (20)$$

where  $l$ ,  $b$ ,  $R_{\text{in}}$  are the variational parameters;  $R_{\text{in}}$  is the radius of the core within which kinetic energy can be neglected, and  $l$  is the characteristic length over which the wave function decays to zero from its constant value of  $b$ . Normalization will fix one of these, say  $b$ , leaving us with two independent variational parameters. Minimizing the energy of the binary system numerically, one can determine the variational parameters. The variational densities using *ansatz* (20) are now in good agreement with the numerical results as illustrated in figures 3(a)-(b).

*Break-down of SMA:* If the condition for the validity of SMA, i.e. the condition  $N_1\sqrt{a_1} = N_2\sqrt{a_2}$ , is not satisfied then the variational analysis discussed above is no longer applicable. For example, considering  $N_1 = N_2 = 50000$  and keeping the interaction parameters same as in figure 2 with both three-body interaction and LHY interaction switched on, the numerical density of the binary ball is shown in figure 4(a). In this case, the densities of the two components are no longer overlapping. The break-down of SMA is much more pronounced in the case with  $N_1 = 50000$ ,  $N_2 = 30000$  as illustrated in figure 4(b). This is because with the parameters of figure 4(b) the violation of the SMA condition  $N_1\sqrt{a_1} = N_2\sqrt{a_2}$  is stronger than with the parameters of figure 4(a).

As mentioned in Sec. 1, both the LHY as well three-body interactions, acting independently or jointly, can stabilize the binary ball. It implies that if three-body interaction coefficient  $K_3$  is assumed to be tunable [37], then by switching off the LHY interaction, one can tune  $K_3$  to obtain a binary ball of similar shape and size as one would obtain with only the LHY interaction. If  $w_0$  is the variational width of the binary ball with only LHY interaction, then using (19), the  $K_3$  needed to obtain the

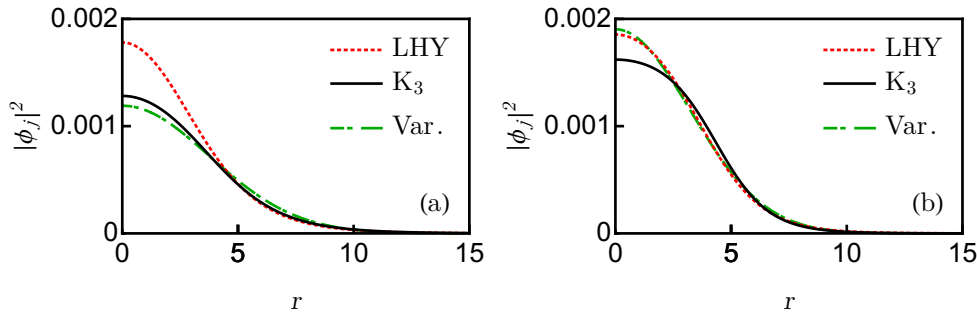


**Figure 5.** Numerical density of a binary  $^{87}\text{Rb}$  ball with (a)  $N_1 = 30000$ , and (b)  $N_1 = 50000$ , with only LHY interaction (LHY) and with only a tuned three-body interaction ( $K_3$ ). The variational density (Var.), which is the same in both cases, is also shown. The tuned  $K_3$ , calculated from (21), is  $2.95 \times 10^{-38} \text{m}^6/\text{s}$  and  $= 1.8 \times 10^{-38} \text{m}^6/\text{s}$  for (a) and (b), respectively. Other parameters used are  $a_1 = 100.4a_0$ ,  $a_2 = 95a_0$ ,  $a_{12} = -105a_0$ , and  $N_2 = N_1 \sqrt{a_1/a_2}$ .

same width with only three-body interaction is

$$K_3 = \frac{2304\sqrt{6}(\sum_i N_i a_i)^{5/2}}{25\sqrt{5}N^3} w_0^{3/2} \pi^{5/4}. \quad (21)$$

For  $N_1 = 30000$ ,  $N_2 = N_1 \sqrt{a_1/a_2}$ ,  $a_1 = 100.4a_0$ ,  $a_2 = 95a_0$ ,  $a_{12} = -105a_0$ , the variational width obtained by using Gaussian *ansatz*, namely (16), with only LHY interaction is  $w_0 = 5.32$ . Using this in (21), the  $K_3$  needed to obtain the same variational width with only three-body interaction is  $2.95 \times 10^{-38} \text{m}^6/\text{s}$ . Similar calculation for  $N_1 = 50000$ ,  $N_2 = N_1 \sqrt{a_1/a_2}$  gives  $K_3 = 1.8 \times 10^{-38} \text{m}^6/\text{s}$ . The numerical and variational results for density with only LHY interaction and with only a tuned three-body interaction are shown in figures 5(a)-(b), which look quite similar.

We also studied the variation of the root-mean-square (rms) sizes of the stationary quantum balls for a fixed number of atoms  $N_1$  as a function of the inter-species scattering length  $a_{12}$  as well as for a fixed  $a_{12}$  as a function of  $N_1$  obtained by a variational, viz. (16), and a numerical solution of the coupled NLS equations (9)-(10) using either an LHY interaction or a tunable [37] three-body interaction  $K_3$ . The variation of the rms sizes of the binary balls, which is same for the two components in SMA, as a function of  $|a_{12}|$  and  $N_1$  when only LHY interaction term is included in NLS equations (9)-(10) is shown in figure 6(a) and figure 6(b), respectively. The same when only the tunable three-body interaction is considered is shown in figures 6(c) and (d). In figures 6 the agreement between variational and numerical results is reasonable. The tunable  $K_3$  is obtained using (21) and gives  $K_3 \sim 10^{-39} - 10^{-38} \text{m}^6/\text{s}$ . We find that either by using only LHY interaction or by using only three-body interaction, binary quantum balls of similar sizes can be obtained as is illustrated in figures 6(a)-(d). Hence for a proper description of the binary ball both the LHY and three-body interactions should be included in the Lagrangian. The values of  $K_3$  used in figures 5 and 6 are a bit large. Nevertheless, there are suggestions for experimentally managing the value of  $K_3$  by external electromagnetic interactions [37], which might provide a way to achieve such large values of  $K_3$ . However, if we take a smaller value of  $K_3$ , a self-bound state will also emerge, which will have a much smaller size.

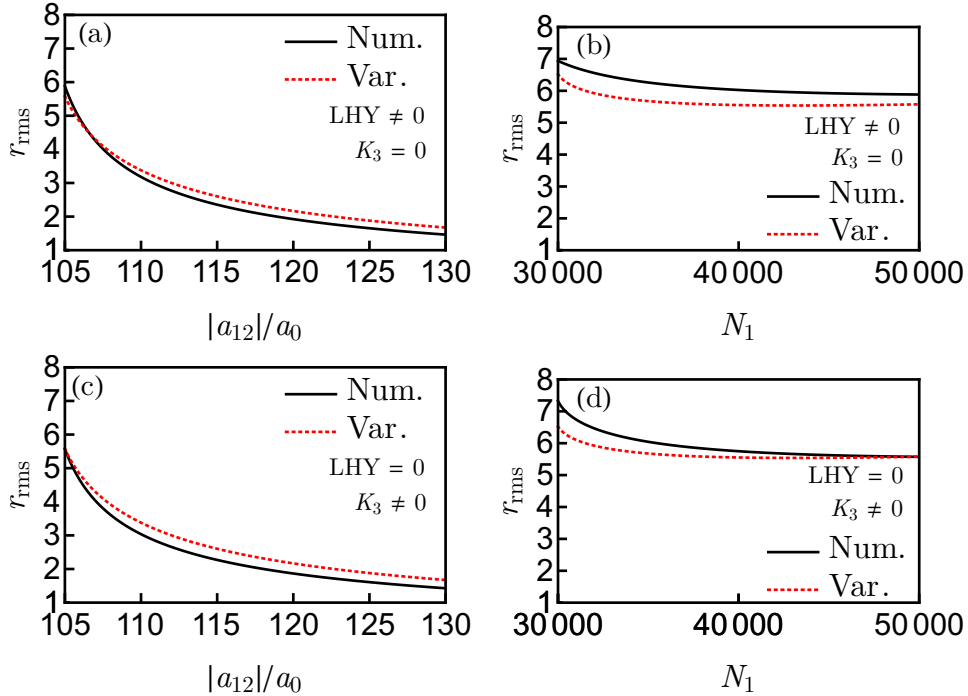


**Figure 6.** (a) Numerical (Num.) and variational (Var.) rms sizes of a binary  $^{87}\text{Rb}$  ball with  $N_1 = 50000$ ,  $K_3 = 0$ , as a function of  $a_{12}$ ; (b) the same as a function of  $N_1$  with  $a_{12} = -105a_0$ ; (c) the same with zero LHY interaction and  $N_1 = 50000$ ,  $K_3 \neq 0$ , tuned using (21), as a function of  $a_{12}$ ; (d) the same with zero LHY interaction as a function of  $N_1$  with  $a_{12} = -105a_0$ ,  $K_3 \neq 0$ , tuned using (21). Other parameters used are  $a_1 = 100.4a_0$ ,  $a_2 = 95a_0$ , and  $N_2 = N_1 \sqrt{a_1/a_2}$ .

### 3.2. Moving quantum balls

To make the quantum balls move with a velocity, say  $v_0$  along  $x$  axis, we multiply the stationary ground-state wave function obtained with imaginary time propagation by  $e^{iv_0x}$ , and evolve this solution in real time. We consider the binary  $^{87}\text{Rb}$  ball shown in figure 2 (a) to study the collision dynamics. To this end, we place two binary balls of figure 2 (a) at  $x = \pm x_0$  and attribute velocities  $v = \pm v_0$  to them so that they collide frontally at  $x = 0$ . We find that the head-on collision is essentially elastic at very large velocities with two balls emerging after collision with no visible deformation in shape. However, as the speed of the colliding binary balls is decreased there is an increased deformation in the shape due to collision. In the opposite extreme of very small velocities, the collision is highly inelastic, and the identity of the two binary balls is lost through the formation of a larger binary ball – a breather or a molecule – in an excited state which stays at the origin ( $x = 0$ ) executing breathing oscillation. The three-body interaction coefficient  $K_3$  is actually complex with a negative imaginary part responsible for the loss of atoms due to three-body recombination. The imaginary part of  $K_3$  in the case of  $^{87}\text{Rb}$  atoms is quite small [34, 36]:  $K_3 = -1.8i \times 10^{-41} \text{ m}^6/\text{s}$ . In the real-time simulation of collisions we consider an identical amount of the real part of  $K_3$ , so that the resultant complex  $K_3$  will be  $1.8(1 - i) \times 10^{-41} \text{ m}^6/\text{s}$ . However,

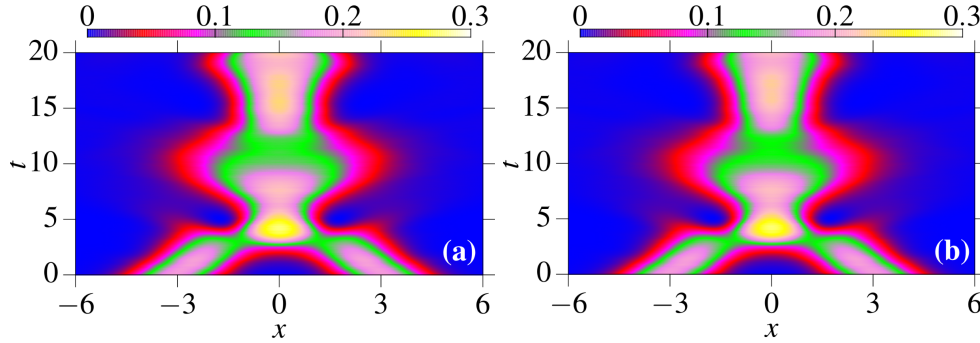


**Figure 7.** The frontal collision of two binary balls of figure 2(a) initially placed at  $x_0 = \pm 3.12$  moving in opposite directions along  $x$  axis with velocity  $v_0 = \pm 0.5$  through a two dimensional contour plot of density  $\sum_{j=1,2} n_j(x, y = 0, z = 0, t)$  in the  $x-t$  plane using (a)  $K_3 = 1.8 \times 10^{-41} \text{ m}^6/\text{s}$  and (b)  $K_3 = 1.8(1-i) \times 10^{-41} \text{ m}^6/\text{s}$ , respectively.

such a small imaginary part of  $K_3$  at a low density of a quantum binary ball of few thousand atoms will lead to a small loss of atoms and would not destroy the essentials of collision dynamics. However, the effect of the inclusion of the imaginary part of  $K_3$  in the calculation of stationary quantum balls of Sec. 3.1 is insignificant. Hence we did not include an imaginary part of  $K_3$  in that calculation. The effect of including an imaginary part of  $K_3$  in collision dynamics is shown in figures 7(a)-(b) for the two binary balls initially placed as  $x_0 = \pm 3.12$  moving with speeds  $v_0 = \pm 0.5$  in opposite directions employing  $K_3 = 1.8 \times 10^{-41} \text{ m}^6/\text{s}$  and  $K_3 = 1.8(1-i) \times 10^{-41} \text{ m}^6/\text{s}$ , respectively. In both cases the two binary balls combine to form an excited breather which oscillates at  $x = 0$ . The difference in density in plots of figure 7 (a) and (b) is not noticeable showing that the recombination loss is negligibly small. In figure 8(a)-(b), we illustrate similar collision of two binary balls at larger velocities  $v_0 = 32$  and  $10$ , respectively. For  $v_0 = \pm 32$ , clean tracks of the binary balls are found to emerge after collision in the  $x-t$  plane indicating the elastic nature of the collision. For  $v_0 = \pm 10$ , the identity of the binary balls is lost after collision as indicated by the diffused trails of the quantum balls after collision.

The quasi-elastic nature of collision of figure 8(a) for  $v = \pm 32$  is illustrated further by snapshots of 3D isodensity contours at different times,  $t = 0, 0.12, 0.16, 0.21, 0.24$  and  $0.32$ , during the collision in figure 9. In case of many atoms the imaginary part of the three-body interaction coefficient  $K_3$  has a larger value corresponding to a larger recombination loss [38]. To see that a larger value of the recombination loss does not destroy the elastic nature of the collision, in this simulation, we consider a  $K_3$  with a large imaginary part:  $K_3 = 1.8 \times 10^{-41}(1-100i) \text{ m}^6/\text{s}$ . The contour plot of the total density  $\sum_j n_j(x, y = 0, z = 0, t)$  in  $x-t$  plane in this case is indistinguishable from that in Fig. 8(a) due to a still smaller recombination loss over a period of  $t = 0.32$ . In (c) the two balls have fully overlapped and formed a unstable larger ball. In (b) and (d) the overlap is partial. The final (f) and initial (a) snapshots of the colliding binary balls look quite similar indicating the elastic nature of the collision.

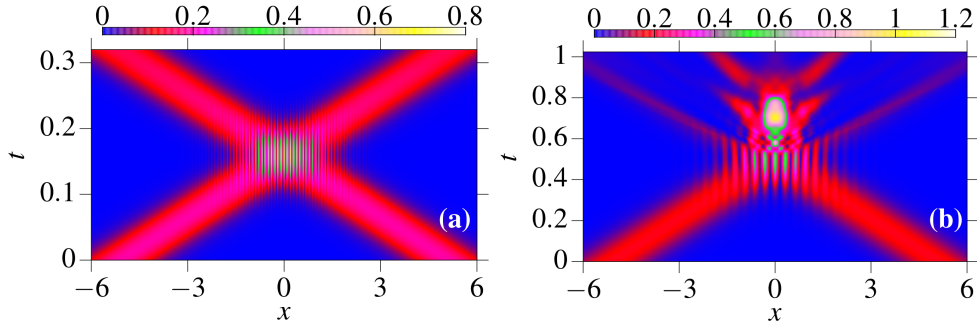


**Figure 8.** The frontal collision of two binary balls of figure 2(a) initially placed at  $x_0 = \pm 5.12$  moving in opposite directions along  $x$  axis with velocity  $v_0 = \pm 32$  and  $\pm 10$  through a two dimensional contour plot of density  $\sum_j n_j(x, y = 0, z = 0, t)$  in the  $x - t$  plane.

#### 4. Summary and discussion

We studied the formation of a binary BEC quantum ball of two hyperfine states of  $^{87}\text{Rb}$  atoms for intra-species repulsion and inter-species attraction in the presence of beyond-mean-field LHY and complex three-body interactions and demonstrate that the LHY and three-body interactions play similar role in the formation of a binary quantum ball. Nevertheless, the strength of the three-body interaction  $K_3$  has to be increased, if the size of the quantum ball stabilized only by the LHY interaction is required to be equal to the same of a quantum ball stabilized only by the three-body interaction. On the other hand, if a smaller value of  $K_3$  is employed the size of the quantum ball will be much smaller. Hence in a comprehensive treatment of the binary BEC quantum ball both these interactions should be included. A similar conclusion was reached on the treatment of a binary boson-fermion quantum ball [9],

In Sec. 2 we derived a set of coupled NLS equations for the binary BEC with two- and three-body interactions and beyond-mean-field LHY interaction. For the formation of a stable binary quantum ball the inter-species interaction is always taken to be attractive and intra-species interaction repulsive. The three-body interaction is taken to be repulsive with an imaginary part responsible for recombination loss. To make the binary NLS equations analytically tractable, we consider a single-mode approximation (SMA) to it valid under some simplifying assumptions on the scattering lengths and number of atoms involved. An analytical Gaussian variational approximation was developed in the SMA. In Sec. 3.1, we performed a numerical solution to the NLS equations in the SMA by imaginary-time simulation and compared the results for stationary binary balls with the corresponding results of variational approximation. We also considered a numerical solution to the binary NLS equations beyond SMA, where there is no analytic variational approximation for a comparison. In Sec. 3.2, the results for collision dynamics obtained by real-time simulation are presented. The elastic collision of two binary balls is found to be elastic at large velocities with practically no deformation of the emerging balls after collision. The collision is inelastic at smaller velocities and at very low velocities the two binary balls combine to form a larger binary ball in an excited state – a breather or a binary-ball molecule – which executes breathing oscillation.

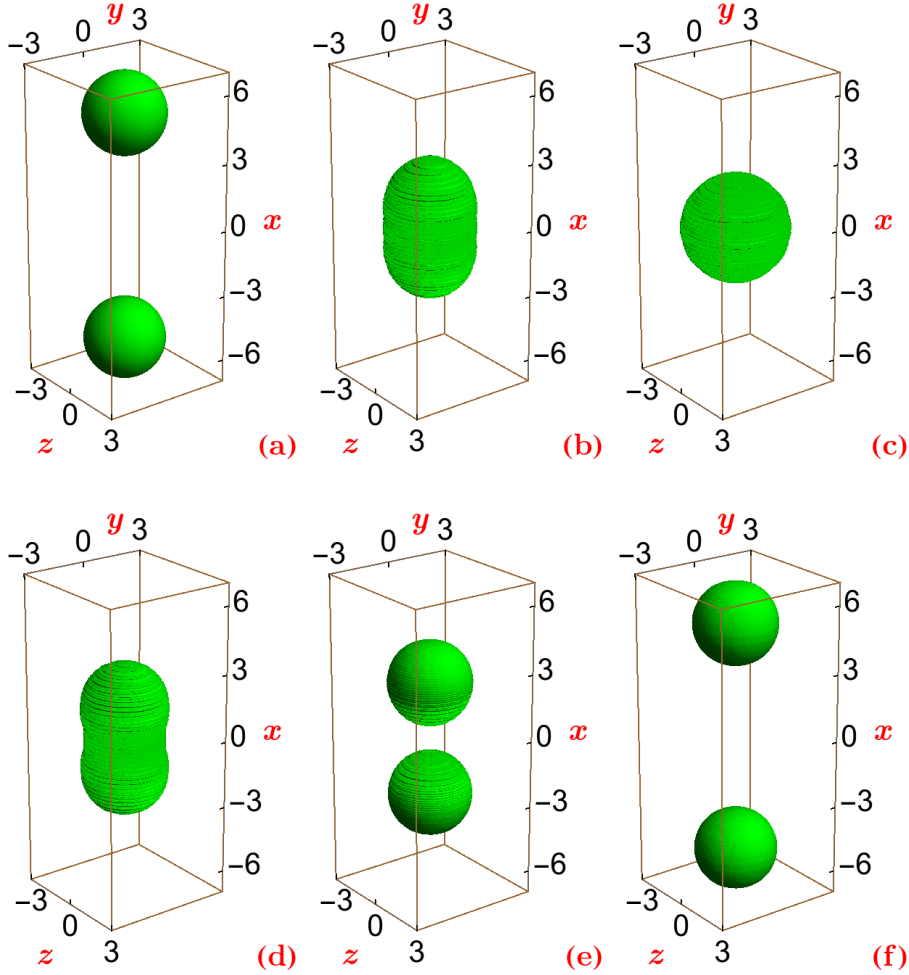


**Figure 9.** Isodensity contours with contour density of 0.02 of the two quantum balls corresponding to dynamics shown in figure 8(a) but calculated with  $K_3 = 1.8 \times 10^{-41}(1 - 100i)$  by real-time simulation at (a)  $t = 0$ , (b)  $t = 0.12$ , (c)  $t = 0.16$  (d)  $t = 0.21$ , (e)  $t = 0.24$ , and (f)  $t = 0.32$ .

After the completion of this study we came to know about a similar investigation [39].

### Acknowledgments

S.K.A acknowledges the support by the Fundação de Amparo à Pesquisa do Estado de São Paulo (Brazil) under project 2016/01343-7 and also by the Conselho Nacional de Desenvolvimento Científico e Tecnológico (Brazil) under project 303280/2014-0.

## References

- [1] Kivshar Y S and Malomed B A 1989 *Rev. Mod. Phys.* **61** 763  
Bagnato V S, Frantzeskakis D J, Kevrekidis P G, Malomed B A and Mihalache D 2015 *Rom. Rep. Phys.* **67** 5  
Mihalache D 2014 *Rom. J. Phys.* **59** 295
- [2] Kivshar Y S and Agrawal G 2003 *Optical Solitons: From Fibers to Photonic Crystals*, (Academic Press, San Diego)
- [3] Strecker K E, Partridge G B, Truscott A G and Hulet R G 2002 *Nature* **417** 150  
Khaykovich L, Schreck F, Ferrari G, Bourdel T, Cubizolles J, Carr L D, Castin Y and Salomon C 2002 *Science* **256** 1290  
Nguyen J H V, Dyke P, Luo D, Malomed B A and Hulet R G 2014 *Nature Phys.* **10** 918  
Cornish S L, Thompson S T and Wieman C E 2006 *Phys. Rev. A* **96** 170401.
- [4] Pérez-García V M, Michinel H and Herrero H 1998 *Phys. Rev. A* **57** 3837  
Abdullaev F K, Gammal A, Kamchatnov A M and Tomio L 2005 *Int. J. Mod. Phys. B* **19** 3415
- [5] Dalfovo F, Giorgini S, Pitaevskii L P and Stringari S 1999 *Rev. Mod. Phys.* **71** 463
- [6] Lee T D and Yang C N 1957 *Phys. Rev.* **105** 1119  
Lee T D, Huang K and Yang C N 1957 *Phys. Rev.* **106** 1135
- [7] Petrov D S 2015 *Phys. Rev. Lett.* **115** 155302
- [8] Adhikari S K 2017 *Phys. Rev. A* **95** 023606
- [9] Adhikari S K 2018 *Laser Phys. Lett.* **15**
- [10] Gautam S and Adhikari S K 2018 *Phys. Rev. A* **97** 013629  
Zhang Y-C, Zhou Z-W, Malomed B A and Pu H 2015 *Phys. Rev. Lett.* **115** 253902  
Li Y, Luo Z, Liu Y, Chen Z, Huang C, Fu S, Tan H and Malomed B A 2018 *New J. Phys.* **19** 113043  
Cappellaro A, Macrì I, Bertacco G F and Salasnich L 2017 *Sci. Rep.* **7** 13358
- [11] Yu Z-F, Zhang A-X, Tang R-A, Xu H-P, Gao J-M and Xue J-K 2017 *Phys. Rev. A* **95**, 033607
- [12] Chen L, Zhu C, Zhang Y and Pu H 2018 *Phys. Rev. A* **97** 031601(R)
- [13] Adhikari S K 2004 *Phys. Rev. A* **86** 063613
- [14] Kadau H, Schmitt M, Wenzel M, Wink C, Maier T, Ferrier-Barbut I and Pfau T 2016 *Nature* **530** 194
- [15] Chomaz L, Baier S, Petter D, Mark M J, Wächtler F, Santos L and Ferlaino F 2016 *Phys. Rev. X* **6** 041039
- [16] Wächtler F and Santos L 2016 *Phys. Rev. A* **93** 061603(R)
- [17] Schmitt M, Wenzel M, Böttcher F, Ferrier-Barbut I and Pfau T 2016 *Nature* **539** 259
- [18] Ferrier-Barbut I, Kadau H, Schmitt M, Wenzel M and Pfau T 2016 *Phys. Rev. Lett.* **116** 215301
- [19] Bisset R N, Wilson R M, Baillie D and Blakie P B 2016 *Phys. Rev. A* **94** 033619
- [20] Wächtler F and Santos L 2016 *Phys. Rev. A* **94** 043618
- [21] Adhikari S K 2017 *Laser Phys. Lett.* **14** 025501
- [22] Cabrera C R, Tanzi L, Sanz J, Naylor B, Thomas P, Cheiney P and Tarruell L 2018 *Science* **359** 301
- [23] Cheiney P, Cabrera C R, Sanz J, Naylor B, Tanzi L and Tarruell L 2018 *Phys. Rev. Lett.* **120** 135301  
Kartashov Y V, Malomed B A, Tarruell L and Torner L 2018 *Phys. Rev. A* **98** 013612
- [24] Semeghini G, Ferioli G, Masi L, Mazzinghi C, Wolswijk L, Minardi F, Modugno M, Modugno G, Inguscio M and Fattori M 2018 *Phys. Rev. Lett.* **120** 235301
- [25] Pérez-García V M, Michinel H, Cirac J I, Lewenstein M and Zoller P 1997 *Phys. Rev. A* **56** 1424
- [26] Gautam S and Adhikari S K 2015 *Phys. Rev. A* **91** 063617
- [27] Muruganandam P and Adhikari S K 2009 *Comput. Phys. Commun.* **180** 1888  
Vudragović D, Vidanović I, Balaž A, Muruganandam P and Adhikari S K 2012 *Comput. Phys. Commun.* **183** 2021  
Young-S L E, Vudragović D, Muruganandam P, Adhikari S K and Balaž A 2016 *Comput. Phys. Commun.* **204** 209  
Satarić B, Slavnić V, Belić A, Balaž A, Muruganandam P and Adhikari S K 2016 *Comput. Phys. Commun.* **200** 411  
Kishor Kumar R, Young-S. L E, Vudragović D, Balaz A, Muruganandam P and Adhikari S K 2015 *Comput. Phys. Commun.* **195** 117  
Lončar V, Young-S. L E, Škrbić S, Muruganandam P, Adhikari S K and Balaž A 2016 *Comput. Phys. Commun.* **209** 190  
V. Lončar, A. Balaž, A. Bogojević, S. Škrbić, P. Muruganandam, and S. K. Adhikari, *Comput.*



- Phys. Commun.* **200**, 406 (2016);
- [28] Bao W and Wang H 2006 *J. of Comput. Phys.* **217** 612  
Muruganandam P and Adhikari S K 2003 *J. Phys. B: At. Mol. Opt. Phys.* **36** 2501  
Wang H 2007 *J. Comput. App. Math.* **205** 88
- [29] Adhikari S K and Gautam S 2018 arXiv:1810.12843
- [30] Adhikari S K and Salasnich L 2008 *Phys. Rev. A* **78** 043616  
Adhikari S K and Salasnich L 2018 *Sci. Rep.* **8** 8825
- [31] Pethick C J and Smith H 2008 *Bose Einstein condensation in Dillute Gases, Second Edition*, (Cambridge University Press, Cambridge).
- [32] Eckardt A, Weiss C and Holthaus M 2004 *Phys. Rev. A* **70** 043615
- [33] Gladush Yu G, Kamchatnov A M, Shi Z, Kevrekidis P G, Frantzeskakis D J and Malomed B A 2009 *Phys. Rev. A* **79** 033623
- [34] Tojo S, Taguchi Y, Masuyama Y, Hayashi T, Saito H and Hirano T 2010 *Phys. Rev. A* **82** 033609
- [35] Inouye S, Andrews M R, Stenger J, Miesner H-J, Stamper-Kurn D M and Ketterle W 1998 *Nature* **392** 151
- [36] Söding J, Guéry-Odelin D, Desbiolles P, Chevy F, Inamori H and Dalibard J 1999 *Appl. Phys. B: Lasers Opt.* **69** 257
- [37] Büchler H P, Micheli A and Zoller P 2007 *Nature Phys.* **3** 726  
Safavi-Naini A, von Stecher J, Capogrosso-Sansone B and Rittenhouse S T 2012 *Phys. Rev. Lett.* **109** 135302  
Huckans J H, Williams J R, Hazlett E L, Stites R W and O'Hara K M 2009 *Phys. Rev. Lett.* **102** 165302  
Petrov D S 2014, *Phys. Rev. Lett.* **112** 103201
- [38] Roberts J L, Claussen N R, Cornish S L and Wieman C E 2000 *Phys. Rev. Lett.* **85** 728
- [39] F. Ancilotto, M. Barranco, M. Guilleumas, and M. Pi 2018 *Phys. Rev. A* **98** 053623